ISSN 1028-334X, Doklady Earth Sciences, 2007, Vol. 415A, No. 6, pp. 954–960. © Pleiades Publishing, Ltd., 2007.
Original Russian Text © M.P. Davydov, P.A. Aleksandrov, E.N. Perova, T.A. Semkova, 2007, published in Doklady Akademii Nauk, 2007, Vol. 415, No. 6, pp. 793–799.

GEOCHEMISTRY

Ferromanganese Deposits in the Ashadze-1 Hydrothermal Field (Mid-Atlantic Ridge, 12°58′ N)

M. P. Davydov[a], P. A. Aleksandrov[a], E. N. Perova[b], and T. A. Semkova[a]

Presented by Academician D.V. Rundqvist July 21, 2006

Received August 30, 2006

DOI: 10.1134/S1028334X07060281

Subaqueous ferromanganese deposits (FMD), except nodules, are commonly classified into hydrogenic and hydrothermal types. According to [1–9 and others], both types are formed as a result of coprecipitation of Fe–Mn colloids that absorb chemical elements, including nonferrous metals (NFM), from seawater. It is assumed that the hydrothermal deposits should be depleted in NFM relative to the hydrogenic counterparts, because the duration of contact of colloids, which produce the hydrothermal deposits, with seawater is much shorter. To subdivide FMD, the diagram (Cu + Ni + Co) × 10 – Fe – Mn proposed by Bonatti et al. [1] is widely used.

However, our investigations have shown that hydrothermal FMD are formed by both coprecipitation of Fe–Mn colloids and direct crystallization of oxyhydroxides from oversaturated solutions. The low NFM contents are only typical of the crusts in the discharge zone of hydrothermal solutions that form hydrothermal-metasomatic (stockwork) sulfide ores. At the same time, the crusts associated with surficial hydrothermal-sedimentary sulfide ore, as a rule, are characterized by very high NFM contents comparable or even exceeding those in FMD [10, 11]. Therefore, the hydrothermal deposits fall into the field of hydrogenic FMD in the Bonatti diagram.

In this communication, based on the study of sediments from the Ashadze-1 hydrothermal field and other original evidence, we substantiate the necessity to recognize hydrothermal-hydrogenic FMD, a new variety of hydrogenic FMC that are deposited near hydrothermal-sedimentary sulfide occurrences. A new discriminant diagram Cu–Cu/Co is proposed for more accurate identification of FMD types in the rift valley of the Mid-Atlantic Ridge (MAR).

The Ashadze-1 hydrothermal field was found in 1993 during cruise 22 of the R/V *Professor Logatchev* in the course of joint survey of the All-Russia Research Institute of Geology and Mineral Resources of the World Ocean (VNIIO) and the Polar Marine Geological Exploration Expedition (PMGRE). The field is located at the edge of a small gentle terrace composed of serpentinized ultramafic and gabbroic rocks at the west wall of the rift valley [12] close to its intersection with a NW-trending lineament. In the study area, this lineament is traced along the western slope of Fersman Seamount, the bend of the rift valley bottom at 12°50′–12°55′ N, and the grabenlike depression in the northern part of the western terrace at 13°00′–13°05′ N (Fig. 1). Beyond this area, the lineament crosses Fersman Seamount (corner uplift) and the transform Marathon Fracture Zone that extends along its southern slope [13, 14].

FMD were found in this field in the central (stations 1021, 1291) and marginal (stations 1087, 1292) sectors of the massive sulfide orebodies, as well as at the surface of hydrothermally altered (often sulfidized and brecciated) serpentinite and gabbro (stations 1007, 1008, 1071, 1085, 1086) in the vicinity of these orebodies.

The mineral composition of samples was studied on DRON-2 and D8 Advance Bruker AXS X-ray diffractometers at St. Petersburg State University and the Institut Français de Recherche pour l'Exploitation de la Mer (IFREMER), France, respectively. The morphology of mineral aggregates was investigated on a JEOL-35 SEM at the Botanical Institute, Russian Academy of Sciences. The bulk chemical composition was determined using the standard technique with chemical analysis and atomic absorption spectroscopy (S-115), the cold vapor method using a PA-915+ analyzer equipped with RP 91C (All-Russia Research Institute of Geology and Mineral Resources of the World Ocean), and the ICP-MS method (All-Russia Geological Research Institute).

[a] *All-Russia Research Institute of Geology and Mineral Resources of the World Ocean, Angliiskii pr. 1, St. Petersburg, 190121 Russia; e-mail: davydov@vniio.ru*

[b] *St. Petersburg State University, Universitetskaya nab. 7/9, St. Petersburg, 199034 Russia*

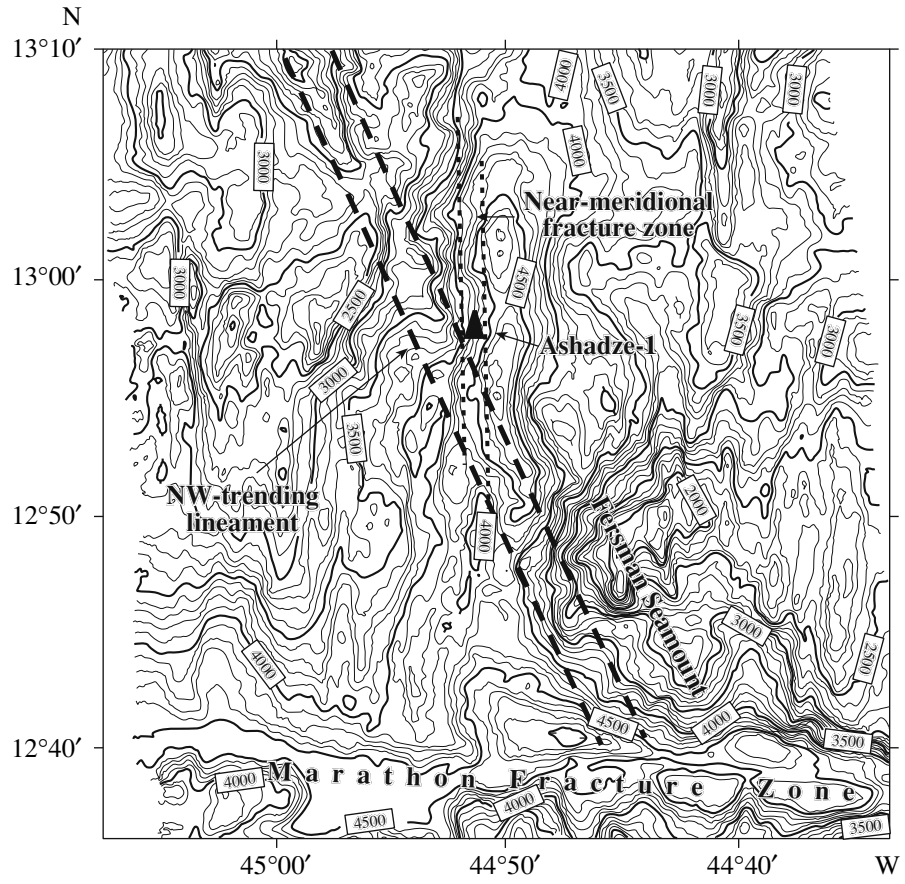

Fig. 1. Index map of the Ashadze-1 high-temperature hydrothermal field.

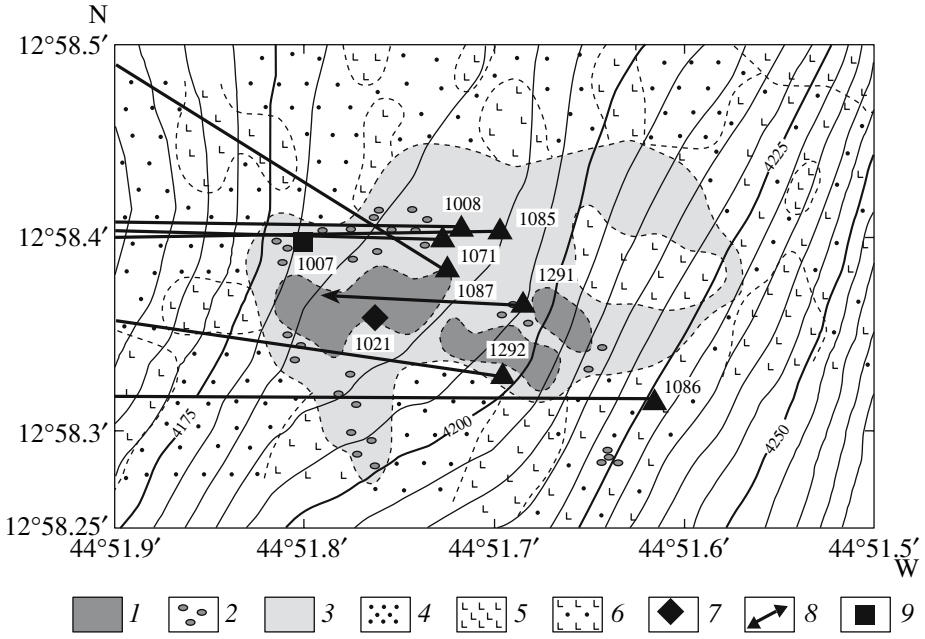

Fig. 2. Geological sketch map of the Ashadze-1 ore occurrence. Modified by N.I. Rozhdestvenskaya and V.E. Bel'tenev after the data of the 22nd, 24th, and 26th cruises of R/V *Professor Logatchev.* (*1*) Sulfide orebody, (*2*) debris of sulfide ore and mineralized rocks, (*3*) ore-bearing and metalliferous mud, (*4*) foraminiferal and coccolithic carbonate sediments, (*5*) bedrock outcrops and fields of large blocks, (*6*) bedrock outcrops and fields of large blocks partly overlapped with sediments; (*7–9*) stations where FMD have been carried up with (*7*) grab, (*8*) dredge, and (*9*) box corer.

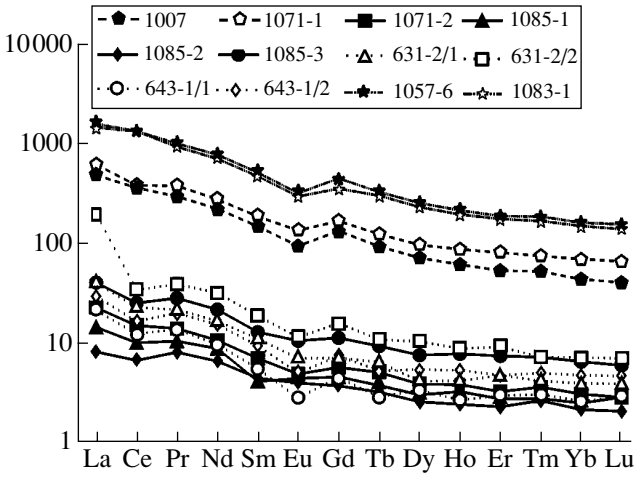

Fig. 3. Chondrite-normalized REE patterns (Taylor and McLennan, 1985) of FMD from Ashadze-1 (stations 1007, 1071, 1085) and Logatchev-2 (stations 631, 643) hydrothermal fields and the western wall of the rift valley (stations 1057, 1083).

Three varieties of FMD recognized in the Ashadze-1 field reveal distinct morphological, structural–textural, chemical, and mineralogical features. The compact sinterlike crusts (2 cm thick) with complex spotty-zonal structure are most abundant. They were identified on sulfide bodies and metasomatic rocks in the marginal area. The following fragments (zones) are recognized in various combinations (from bottom to top): (i) yellow-orange, rust-colored powdery and feltlike bacteriomorphic masses of goethite often with kidney-shaped FMD that envelop goethite fragments (1–2 mm); (ii) intergrowths of gray massive thin-bedded, complexly convoluted and kidney-shaped, fingerlike birnessite segregations, often together with black and brown powdery amorphous segregations of Fe–Mn hydroxides and less abundant goethite (0.5–1.5 cm); and (iii) bunchy intergrowths of birnessite and black and brownish black amorphous Fe–Mn hydroxides (2–3 mm). The vertical and lateral boundaries between the zones are diffuse. Pseudomorphs of Fe–Mn oxyhydroxides after polychaetas are abundant. Sporadic pseudomorphs after diatoms and sponge spicules are noted. The manganese minerals are locally replaced with an amorphous Fe–Si substance. In marginal sectors of such areas, the black manganate aggregates become reddish. They are gradually dissolved inward and replaced with red-brown powdery and less frequent compact glassy Fe–Si masses with abundant bacteriomorphic goethite. The bunchy aggregates are replaced most readily, whereas the massive variety is more stable.

The second variety of FMD was recovered together with aragonitized and serpentinized ultramafic rocks (Station 1086). These sinterlike crusts are up to 1.5 cm thick. Their slightly convex surface is rough. The concave bottom is covered by mm-scale coating of bacteriomorphic goethite or cherry-colored powdery amorphous mass. The structure is zonal. The lower zone (1 cm thick) has a framework that consists of thin (up to 1 mm) entangled beds of black and cherry brown compact mass of 10-Å minerals (todorokite $NaMn_6O_{12} \cdot 3H_2O$ with an admixture of vernadite $Mn(OH)_4$ and birnessite). The fingerlike aggregates of pyrochroite $Mn(OH)_2$ and lithiophorite $(Al,Li)MnO_2(OH)_2$ of the same color grow out of these beds to meet one another like stalactites and stalagmites(!). In some cases, they fill the interlayer space completely, and a free space is left in other cases. The areas filled with powdery and kidney-shaped aggregates are much less frequent. Discrete crystals, coatings, and radiate aragonite aggregates are located in cavities. The upper zone up to 7 mm thick consists of compact carbonated sediment (aragonite, calcite, and manganocalcite) with black and cherry brown globules of Ca-todorokite $[(Mn,Ca)Mn_5O_{11} \cdot 4H_2O]$ occasionally intruded by the underlying material.

The third variety of FMD is composed of thin (up to 1 mm) loose globular and bunchy coatings of amorphous Fe–Mn oxyhydroxides that cover fragments of serpentinized ultramafic rocks (samples 1007, 1071-1).

The above varieties differ in chemical composition (table; Fig. 3). The compositions of the crust from the Logatchev-2 field and FMD from the wall of the rift valley to the west of the Ashadze-1 ore occurrence (stations 1057, 1083) are presented for comparison. For example, crusts of the first variety are characterized by elevated contents of K, Na, Mn, Cu, Zn, Mo, Li, and subordinate Cd. In this regard, they are close to the todorokite–birnessite crusts from the Logatchev-2 field. The variety of carbonates is appreciably distinguished by anomalously high Ca and Mg contents and anomalously low Fe, Ni, Co, Zn, Pb, and W contents. This sample contains much less K, Na, Mn, Cu, Mo, Tl, and Li, but the content of Cu is nevertheless higher than that of other NFMs. In terms of the REE pattern, both varieties, like the crusts from the Logatchev-2 field, pertain to the hydrothermal type [5, 6] with the low total REE content and low negative Ce anomaly (Ce/Ce*). Minor amounts of S_{tot} and Hg indicate that the elevated Cu content is not related to sulfides.

The third variety is characterized by high Fe, Co, and Pb contents and depletion in Mn. This variety is close to the hydrogenic deposits at the western wall in terms of contents of Mn, Fe, Co, Zn, and Pb and to the hydrothermal crusts of the first variety in terms of Cu and Ni contents. In contrast to samples 1057 and 1083 with the high content of total REE and Ce/Ce* > 1 (typical of the hydrogenic variety), the loose sediments are characterized by a lower content of the total REE and Ce/Ce* < 1. In other words, in terms of the REE pattern, they occupy a transitional position between hydrothermal and hydrogenic FMD [5, 6]. The enrichment of hydrothermal crusts in Mn and Cu and their depletion in Al and Pb (against the high background contents of Fe and Co in hydrogenic deposits) make it possible to use Mn/Fe, SiO_2/Al_2O_3, Cu/Co, and (Cu + Zn)/(Co + Pb)

Chemical composition of ferromanganese deposits (FMD)

Component	Hydrogenic FMD from the west wall	FMD from the Ashadze-1 field												Hydrothermal FMD from the Logatchev field
		hydrothermal-hydrogenic			hydrothermal									
		1007	1071-1	Average	1008*	1021-2	1071-2	1085*	1086	1087*	1291	1292	Average**	
SiO_2	8.02 (12)				4.73 (5)	7.40	7.00	2.47 (5)	2.15	5.22 (6)	2.15	2.33	4.31 (20)	3.91 (5)
TiO_2	0.80				0.05	0.07	0.16	0.08	0.10	0.08			0.08	0.14
Al_2O_3	2.33				0.38	0.98	1.02	0.87	1.14	1.13			0.83	0.95
MgO	2.16				2.04	5.25	1.95	2.32	5.88	2.73			2.52	2.13
K_2O	0.30				0.72	0.74	0.50	0.78	0.25	0.68			0.71	0.95
CaO	4.74				1.54	2.40	1.70	2.13	24.4	2.26			2.00	2.32
Na_2O	1.49				4.09	3.08	4.51	4.30	0.96	4.16			4.14	3.08
S_{tot}	0.19				0.09	0.02	0.02	0.19	0.09	0.11	0.04	0.03	0.11	0.01
Mn	8.55	6.47	11.23	8.85	36.90 (6)	34.93	39.19	43.09 (6)	24.16	39.26	36.45	37.27	38.70 (22)	32.92
Fe	25.60	15.39	16.62	16.01	6.23	5.41	1.68	2.65	0.40	5.26	2.41	1.08	4.36	1.17
Cu	535	1400	5200	3300	1710	3000	4100	2283	350	4950	12000	1000	3353	52460
Ni	797	1100	1900	1500	750	580	1300	1292	50	658	770	2700	980	762
Co	1514	700	1900	1300	450	300	500	667	50	667	1000	290	581	256
Zn	496	300	520	410	617	2200	640	663	30	780	1100	310	755	1456
Pb	546	300	450	375	83	50	50	50	50	50	7	7	55	15
Cd	0.07 (2)						0.05	0.26	0.05				0.22 (4)	9.25 (2)
Mo	139						173	301	73				269	600
W	80.8						10.10	4.78	0.91				6.11	15.40
Sn	16.5						5.50	4.17	5.11				4.50	7.55
Tl	16.55						8.78	9.93	1.04				9.65	37
Li	13.24						643	725	316				705	415
Sr							194	300	100				274	545
Hg	25 (8)				18 (4)	21	16	24 (5)	20	56			33 (17)	9

Table. (Contd.)

Component	Hydrogenic FMD from the west wall	FMD from the Ashadze-1 field												Hydrothermal FMD from the Logatchev-2 field
		hydrothermal-hydrogenic			hydrothermal									
		1007	1071-1	Average	1008*	1021-2	1071-2	1085*	1086	1087*	1291	1292	Average**	
La	565 (2)	180	230	205			8.45	7.84 (3)	4.15				7.84 (4)	44.50 (2)
Ce	1290	350	370	360			14.50	13.55	6.64				13.55	27.50
Pr	135	41.10	52.70	46.90			1.95	2.16	0.92				2.16	4.20
Nd	535	160	200	180			7.66	8.89	3.33				8.89	17.50
Sm	115	34.60	43.40	39			1.64	1.67	0.62				1.67	3.50
Eu	27.05	8.27	11.90	10.09			0.43	0.56	0.17				0.56	0.81
Gd	125	41.30	51.80	46.55			1.77	2.02	1.14				2.02	3.35
Tb	18.60	5.50	7.26	6.38			0.30	0.32	0.11				0.32	0.51
Dy	94.05	27.60	37.30	32.45			1.49	1.69	0.62				1.69	2.80
Ho	17.70	5.28	7.49	6.39			0.33	0.39	0.12				0.39	0.56
Er	45.90	13.40	20.40	16.90			0.82	1.05	0.30				1.05	1.75
Tm	6.37	1.88	2.71	2.30			0.13	0.15	0.05				0.15	0.21
Yb	39.25	11	17.50	14.25			0.77	0.94	0.29				0.94	1.40
Lu	5.68	1.56	2.56	2.06			0.11	0.14	0.04				0.14	0.21
Mn/Fe	0.33	0.42	0.68	0.55	7.47	6.46	23.33	30.43	60.61	9.46	15.12	34.51	16.53	102.17
SiO_2/Al_2O_3	3.14				16.56	7.55	6.86	3.03	1.89	4.64			7.79	4.47
Cu/Co	0.36	2.00	2.74	2.37	3.80	10.00	8.20	3.42	7.02	7.42	12.00	3.45	5.68	233.18
(Cu + Zn)/(Co + Pb)	0.51	1.70	2.43	2.07	4.46	14.86	8.62	4.18	3.80	8.40	13.01	4.41	6.50	212.54
REE total	1855	882	1055	968			40.35	41.36	18.50				41.10	109
Ce/Ce*	1.10	0.95	0.79	0.87			0.84	0.80	0.80				0.81	0.58
Eu/Eu*	0.69	0.67	0.77	0.72			0.77	0.96	0.62				0.91	0.73
Ce*/Eu*	1.58	1.43	1.03	1.23			1.09	0.83	1.29				0.89	0.78

Note: Major elements (SiO_2–Fe) are given in wt %; trace elements (Cu–Sr and REE), in ppm; Hg, in ppb. Analytical methods: chemical analysis for major elements, AAS for Pb, cold vapor method for Hg, and ICP-MS for other trace elements. The averaged data are denoted by one asterisk; average values without data from Station 1086, by two asterisks. The number of analyses is given in parentheses. (Ce*) Geometric mean between La and Pr; (Eu*) geometric mean between Sm and Gd.

ratios for discrimination of these FMD types. In terms of these parameters, the deposits of the third type are transitional as well (table).

The prevalence of Cu over Co is inherent to FMD from other hydrothermal fields of the MAR with occurrences of hydrothermal-sedimentary sulfide ore. Such a feature was not established in the hydrothermal-metasomatic ore occurrences, where Zn often predominates among the NFMs [10, 11]. At the same time, most hydrogenic deposits in the MAR are distinguished by relatively high Co contents [9–11]. This difference confirmed by statistical processing of more than 300 analyses [11] is distinctly expressed in the Cu vs. Cu/Co diagram (Fig. 4), where compositions of 98 FMD samples from 52 stations in the MAR rift valley have been plotted. Four groups of FMD are recognized.

The crustlike FMD of the first and second groups are referred to as a hydrothermal type. Their relations to the hydrothermal sulfide formation are corroborated by dredging. The hydrothermal crusts characterized by a high growth rate were formed under nonequilibrium conditions at the hydrothermal solution–seawater geochemical barrier (as sulfide ore). Judging from the textural–structural features, these crusts are products of direct crystallization of manganese minerals from oversaturated solutions rather than products of avalanche-like coprecipitation of Fe–Mn colloids as was supposed previously. In the course of crystallization, K, Na, Co, Ni, Cu, Zn, Mo, Li, Cd, and other elements are incorporated into the lattice of manganates. At some moments of the hydrothermal cycle, the density of ore-bearing solutions became higher than that of seawater (sols) and these solutions spread from a vent at the bottom as stratified branching microflows (streams). It is suggested that the gray massive bedded segregations were formed as products of crystallization of such microflows. The intercalating fingerlike, bunchy, and kidney-shaped aggregates are products of manganate crystallization from less dense solutions diluted with seawater. Only powdery amorphous masses were probably formed by coagulation of the dissolved Fe and Mn species.

The geochemical features allow us to suggest that the crusts of the first group grew at the sites of discharge of hydrothermal solutions with low concentrations of Cu and other NFMs. Therefore, they are depleted in these elements (except Zn in some cases). The crusts of the second group grew at the sites with high NFM concentrations in solution with predominance of Cu and/or Zn and are enriched in these metals. Furthermore, the NFM contents in hydrothermal crusts are controlled by their mineral composition. In contrast to other manganese oxyhydroxides, the total NFM contents in 10-Å manganates may attain 8% of Mn^{2+} concentration [15]. The 10-Å manganates crystallize simultaneously with the hydrolysis of Mn^{2+} cations and NFM. This process is promoted by high pH (>8) and moderate oxidizing potential. As follows from the prevalent todorokite–birnessite composition, the hydrothermal crusts grow

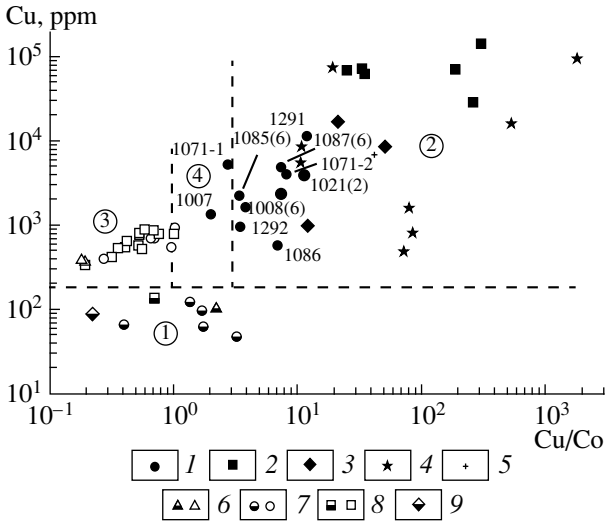

Fig. 4. Compositions of FMD from the rift valley of the equatorial segments of the MAR plotted on the discriminant diagram Cu vs. Cu/Co. Hydrothermal fields: (*1*) Ashadze-1, (*2*) Logatchev-1, Logatchev-2, (*3*) Lucky Strike, (*4*) TAG (Mir), (*5*) Snake Pit; segments of rift: (*6*) 6° N (Markov Basin), (*7*) 13°–15° N, (*8*) 16°–17° N, (*9*) 24°30′ N. Numerals in circles: (1) hydrothermal crusts that mark hydrothermal-metasomatic sulfide ore; (2) hydrothermal crusts that mark hydrothermal-sedimentary sulfide ore; (3) hydrogenic FMD; (4) cupriferous hydrogenic (hydrothermal-hydrogenic) FMD.

under slightly alkaline and low-oxidizing conditions. If Ca activity is high enough, coprecipitation of carbonates and manganates is possible under such conditions. If the parameters of hydrothermal solutions change to slightly acid and low-reducing ones, manganese aggregates are replaced with Fe–Si compounds.

The loose FMD of the third and fourth groups are formed in the principally distinct, hydrogenic mode by coprecipitation of Fe–Mn colloids. Therefore, FMD of both types are enriched in chemical elements absorbed from seawater. In deposits of the fourth group, Cu prevails over Co. In the Cu–Cu/Co diagram, their compositions occupy a space between the typically hydrogenic FMD of the third group and the crusts of high-temperature hydrothermal fields, and thus may be called hydrothermal-hydrogenic. The hydrothermal-hydrogenic FMD are a variety of cupriferous hydrogenic deposits developed in the Cu-rich hydrochemical fields. The local concentration of Cu in the bottom water may be related to different causes. Under conditions of a rift valley, i.e., in the absence of thick sedimentary cover, the most probable mechanism is the discharge of Cu-bearing solutions, including the solutions that produce hydrothermal-sedimentary sulfide ores. This fact makes it possible to use the hydrothermal-hydrogenic FMD as a prospecting guide for sulfide ores.

ACKNOWLEDGMENTS

We thank the staff of the Polar Marine Geological Exploration Expedition and specifically V.E. Bel'tenev

for assistance in collecting factual data and for partial funding of analytical procedures. We are also grateful to the colleagues from IFREMER for the opportunity of working on a D8 Advance Bruker AXS diffractometer.

This work was supported by the Ministry of Natural Resources of the Russian Federation.

REFERENCES

1. E. Bonatti, T. Kraemer, and H. Rydell, in *Ferromanganese Deposits on the Ocean Floor* (Natur. Sci. Foundation, Washington, 1972), pp. 149–165.
2. J. B. Corliss, J. Dymond, M. Lyle, et al., Earth Planet. Sci. Lett. **40**, 12 (1978).
3. J. B. Toth, Geol. Soc. Am. Bull. **91**, 44 (1980).
4. Yu. A. Bogdanov, L. P. Zonenshain, A. P. Lisitsyn, et al., Izv. Akad. Nauk SSSR, Ser. Geol., No. 7, 103 (1987).
5. I. I. Volkov and A. V. Dubinin, Litol. Polezn. Iskop, **22** (6), 40 (1987).
6. G. N. Baturin, L. V. Dmitriev, E. E. Rakovsky, et al., Geokhimiya **27**, 592 (1989).
7. A. Usui, M. Bau, and T. Yamazaki, Mar. Geol. **141**, 269 (1997).
8. R. A. Mills, D. B. Wells, and S. Roberts, Chem. Geol. **176**, 283 (2001).
9. E. S. Bazilevskaya, S. G. Skolotnev, and Yu. M. Pushcharovsky, Dokl. Earth Sci. **377A**, 288 (2001) [Dokl. Akad. Nauk **377**, 516 (2001)].
10. M. P. Davydov, R. V. Goleva, E. N. Perova, et al., Dokl. Earth Sci. **390**, 473 (2003) [Dokl. Akad. Nauk **390**, 70 (2003)].
11. M. P. Davydov, in *Minerals of the Ocean Integrated Strategies-2* (VNIIOkeangeologiya, St. Petersburg, 2004), p. 129.
12. V. Beltenev, A. Nescheretov, V. Shilov, et al. Int. Ridge News **12** (1), 13 (2003).
13. A. O. Mazarovich, *Geology of the Central Atlantic: Faults, Volcanic Edifices, and Deformation of the Oceanic Floor* (Nauchnyi Mir, Moscow, 2000) [in Russian].
14. J. Escartin, D. K. Smith, and M. Cannat, Geophys. Res. Lett. **30**, 1620 (2003). doi: 10.1029/2003GL017226.
15. S. Roy, *Manganese Deposits* (Academic Press, London, 1981; Mir, Moscow, 1986).